Journal of the American College of Cardiology
© 2010 by the American College of Cardiology Foundation
Published by Elsevier Inc.

Vol. 55, No. 16, 2010
ISSN 0735-1097/10/$36.00
doi:10.1016/j.jacc.2010.01.021

Pathological Findings at Bifurcation Lesions

The Impact of Flow Distribution on Atherosclerosis and Arterial Healing After Stent Implantation

Gaku Nakazawa, MD,* Saami K. Yazdani, PHD,* Aloke V. Finn, MD,† Marc Vorpahl, MD,* Frank D. Kolodgie, PHD,* Renu Virmani, MD*

Gaithersburg, Maryland; and Atlanta, Georgia

Objectives Using human pathologic specimens from the CVPath registry, we aimed to investigate the location of the atherosclerotic plaque at bifurcation in native coronary atherosclerotic lesions and to determine the responses at bifurcation after implantation of bare-metal stents (BMS) and drug-eluting stents (DES).

Background Greater atherosclerotic plaque burden has been reported to occur at low-shear regions of bifurcation.

Methods Twenty-six randomly selected human atherosclerotic nonstented coronary bifurcation lesions were examined longitudinally for plaque distribution in patients dying of severe coronary artery disease. Forty stented bifurcation lesions (21 BMS and 19 DES) were reviewed and analyzed by morphometry.

Results In nonstented coronary bifurcations, the lateral wall showed significantly greater intima as well as necrotic core thickness than the flow divider. In the stented lesion, the frequency of late stent thrombosis was greater in the DES group (75%) than in the BMS group (36%), whereas restenosis was more frequent in the BMS group (33%) than in the DES group (5%). Neointimal formation was significantly less at the flow divider compared with the lateral wall in the DES group (0.07 mm [interquartile range (IQR) 0.03 to 0.15 mm] vs. 0.17 mm [IQR 0.09 to 0.23 mm]; $p = 0.001$), whereas this difference was not significant in the BMS group. Similarly, uncovered struts and fibrin deposition was significantly greater at the flow divider compared with the lateral wall in the DES group (uncovered: 40% [IQR 16% to 76%] vs. 0% [IQR 0% to 15%]; $p = 0.001$; fibrin: 60% [IQR 21% to 67%] vs. 17% [IQR 0% to 55%]; $p = 0.01$), but not in the BMS group.

Conclusions Plaque formation in native coronary bifurcations and neointimal growth after DES implantation was significantly less at the flow divider versus the lateral wall. A higher prevalence of late stent thrombosis in DES compared with BMS was associated with greater uncovered struts at flow divider sites, which is likely due to flow disturbances. (J Am Coll Cardiol 2010;55:1679–87) © 2010 by the American College of Cardiology Foundation

Atherosclerotic lesions tend to form at specific regions of the coronary vasculature where flow is disturbed, particularly in areas of low shear (1–3). Because dramatic hemodynamic alternations occur at branch points within the arterial tree, coronary bifurcations are extraordinarily susceptible to atherosclerosis. Areas of low-shear stress are thought to accelerate atherosclerosis through modulation of gene expression, including the promotion of endothelial cell dysfunction, which causes increased uptake of lipoproteins, upregulation of leukocyte adhesion molecules, and leukocyte endothelial transmigration, all of which contribute to the development and progression of atherosclerosis (4).

It is estimated that coronary bifurcation lesions are involved in up to 10% of all percutaneous coronary interventions (PCIs) (5). Early results using bare-metal stents (BMS) to treat bifurcation lesions resulted in a high angiographic acute success rate, but were limited by a higher rate of restenosis (6,7). Although the use of drug-eluting stents (DES) has reduced restenosis rates in bifurcation lesions, long-term outcomes are tempered by an increased risk for thrombosis (8), which raises the possibility that delayed healing seen after DES implantation may be exacerbated at bifurcation sites, perhaps secondary to stent-

From the *CVPath Institute, Inc., Gaithersburg, Maryland; and the †Department of Cardiology, Emory University School of Medicine, Atlanta, Georgia. Dr. Finn has received a research grant from Boston Scientific. Dr. Virmani has received research support from 3F Therapeutics, Abbott Vascular, Amaranth Medical, Inc., Apnex Medical, Ardian, Inc., Atrium Medical Corporation, CardioDex, Ltd., CardioKinetix, Inc., CorAssist Cardiovascular, Ltd., Cordis Corporation, Devax, Inc., ev3, Gardia Medical, Ltd., GlaxoSmithKline, HemCon, Lutonix, Inc., Medtronic Vascular, Meril Life Sciences Pvt, Ltd., Microvention, Inc., Novartis Pharmaceuticals Corporation, NovoStent Corporation, Oregon Medical Laser Center, Prescient Medical, Inc., Relisys Medical Devices Limited, Vascular Therapies, LLC, and Xtent, Inc.; and is a consultant to Medtronic AVE, Abbott Vascular, W. L. Gore, Volcano Therapeutics, Inc., Prescient Medical Inc., CardioMind, Inc., Direct Flow, and Atrium Medical Corporation.

Manuscript received August 7, 2009; revised manuscript received October 20, 2009, accepted January 20, 2010.

Abbreviations and Acronyms

BMS = bare-metal stent(s)
DES = drug-eluting stent(s)
PCI = percutaneous coronary intervention

induced flow disturbances in combination with locally eluted drugs.

The aim of the present study was to determine the role of shear stress on plaque formation at bifurcation sites and the influence of flow patterns in stented coronary arteries. We assessed the anatomic distribution of atherosclerotic plaque in human coronaries using the CVPath Sudden Cardiac Death Registry and compared the pathologic arterial response with bifurcation stenting with DES and BMS cases from the CVPath stent registry.

Methods

Patient population. From the CVPath Sudden Cardiac Death Registry, nonstented bifurcation lesions that had been cut longitudinally were examined in patients dying of sudden cardiac death with severe coronary artery disease (more than 75% stenosis in 1 or more epicardial coronary arteries). For stented lesions, the CVPath Stent Registry was reviewed to select bifurcation lesions that had been treated with DES and BMS (collected from 1999 to 2008). For the case to be included as a bifurcation lesion in the stent study, the main branch stent had to be located in a major epicardial coronary artery and the stented segment had to include a side branch diameter of 2 mm or more in diameter.

Histologic preparation. All specimens had been perfusion fixed at 100 mm Hg with 10% buffered formalin. Hearts were X-rayed and then the epicardial coronary arteries were dissected off the heart and reradiographed. Nonstented arteries were submitted for paraffin embedding and were cut longitudinally. Stented arteries were submitted for plastic embedding and were cross sectioned serially at 2- to 3-mm intervals. Also, proximal and distal nonstented coronary arteries were dehydrated and were embedded in paraffin for further examination. All sections were stained with hematoxylin and eosin and Movat pentachrome as described previously (9,10).

Pathologic assessment and morphometric analysis. In nonstented coronary bifurcation lesions, the intimal thickness was measured and compared among the different locations, that is, the lateral wall of the main branch (proximal and distal to bifurcation), the flow divider region of the main and side branch, and the lateral wall of the side branch (Fig. 1A). Similarly, necrotic core thickness also was measured.

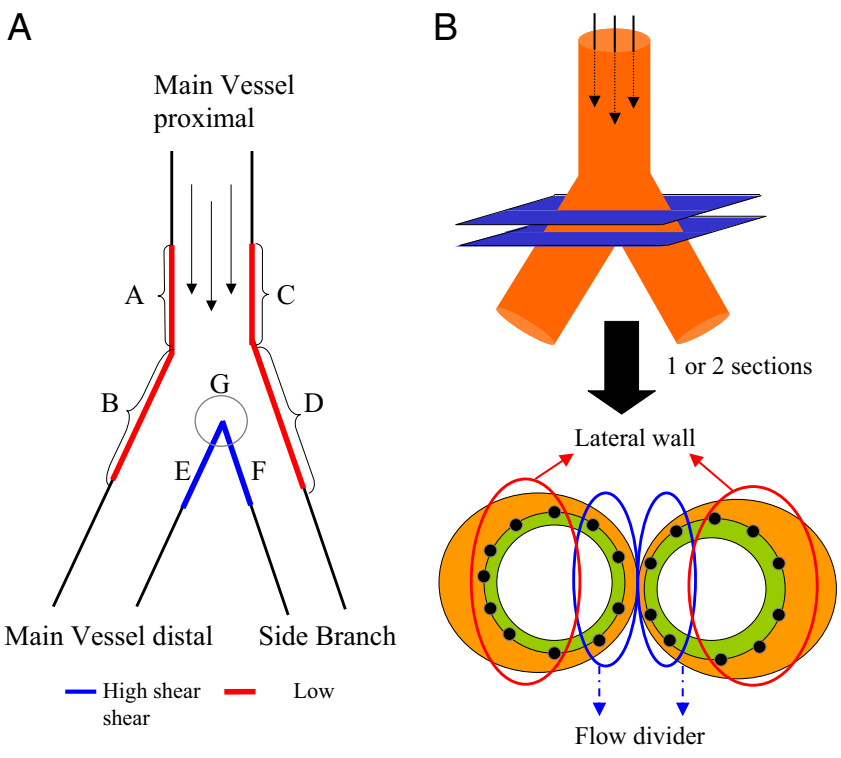

Figure 1 Morphometric Analysis

(A) Illustration showing how, for nonstented atherosclerotic lesions, sections were assessed based on the longitudinal location: A, proximal main vessel; B, distal main vessel on the lateral wall; C, proximal main vessel on the branch side; D, distal side branch on the lateral wall; E, distal main vessel on the flow divider side; F, distal side branch on the flow divider side; G, carinal area. **(B)** Illustration of the method of sectioning of the main and side branch cross sections in the bare-metal stents and drug-eluting stents with regions of interest (flow divider and lateral wall).

In stented lesions, the presence of acute thrombus was defined as a platelet-rich thrombus that occupied more than 30% of the cross-sectional area of the lumen, and restenosis was defined as a more than 75% cross-sectional area narrowing by neointimal formation as reported previously (10). Stent-related death was defined as either related to stent thrombosis or restenosis or to procedure-related death (i.e., coronary perforation, dissection). Nonstent-related cardiac death was defined as a patent stent without evidence of thrombus or restenosis in association with 1 or more nonstented major coronary artery stenosis (cross-sectional area narrowing of more than 75%) or presence of congestive heart failure, valvular heart disease, or both.

To assess the impact of flow disturbance on arterial healing in stented lesions, the differences between flow divider and lateral wall sites were compared (Fig. 1B). Neointimal thickness above the stent struts was defined as the mean thickness between luminal surface of the strut and vessel lumen, which was measured using calibrated software (IPLab, BD Bioscience Bioimaging, Rockville, Maryland). The number of stent struts surrounded by fibrin deposition was recorded, and the percent of struts with fibrin was calculated by the following formula: (number of struts with fibrin/total struts number in the region) × 100. An uncovered strut was defined as a stent strut without neointimal coverage, surface endothelium, or both, and the ratio of uncovered to total stent struts per section was calculated as described previously (11). All parameters were recorded separately in flow divider and lateral wall sites, respectively.

In vitro flow model. To determine the effects of a stent on flow disturbances, a transparent elastomeric silicone (Sylgard 184, Dow Corning Corporation, Midland, Missouri) with an inner diameter of 3.2 mm, wall thickness of 0.5 mm, and an angle of 40° was created (12). The bifurcation model was positioned within a closed-flow loop system consisting of a computer-controlled gear pump, flow reservoir, and flow constrictors. An ultrasonic flow meter (Transonic Systems, Inc., Ithaca, New York) and pressure transducer catheter system (Millar Instruments, Inc., Houston, Texas) were used to monitor the pulsatile flow conditions. Flow constrictors downstream of the bifurcation were adjusted to create a 65:35 split ratio of flow through the daughter tubes. To visualize the flow, the circulating media was seeded with neutrally buoyant glass sphere particles (18 μm; Potters Industries, Inc., Valley Forge, Pennsylvania), excited with a 125-mW green laser (Dragon Lasers, ChangChun, China), and captured using a fast CMOS digital camera (600 frames/s; Vision Research, Wayne, New Jersey). A balloon-expandable BMS (3.0 × 12 mm; Multi-Link Vision, Abbott Vascular, Santa Clara, California) was inflated to a final diameter of 3.5 mm within the bifurcation model, followed by side branch dilatation with final kissing balloon inflation for 20 seconds. The flow conditions of our system mimicked that of native human arterial circulation with a mean Reynolds number of 436 (66 ml/min) and a Womersely parameter of 4.00 (60 beats/min), with pressure ranging from 60 to 120 mm Hg, which corresponds to physiological conditions. The Reynolds and Womersely numbers are nondimensional parameters that govern flow characteristics and are used to mimic similar hemodynamic environments between native arteries and modeling systems.

Statistical analysis. Normally distributed continuous variables are expressed as mean ± SD. Discrete variables and continuous variables with non-normal distribution were expressed as median and interquartile range. Comparisons of plaque and necrotic core thickness between each location were performed using the paired *t* test. Comparison between the DES and BMS groups were tested by the Student *t* test for normally distributed continuous variables and the Fisher exact test for categorical variables. The Wilcoxon rank-sum test was used for comparison of non-normally distributed parameters and discrete variables. The Wilcoxon signed-rank test was used for comparisons of neointimal thickness, percent of struts with fibrin deposition, and percent of uncovered struts between flow divider versus lateral wall site within the same lesion. No corrections were made for correlated observations within the same individuals. The normality of distribution was tested with the Wilk-Shapiro test. A value of $p < 0.05$ was considered statistically significant.

Results

Analysis for nonstented bifurcation lesions (atherosclerosis). Twenty-six bifurcation lesions in 18 patients (male; 88%) dying of severe coronary artery disease were examined (left main/left anterior descending coronary artery/left circumflex = 5; left anterior descending coronary artery/left diagonal = 14; left circumflex/left obtuse marginal = 5; left circumflex/posterior descending = 1; right coronary artery/posterior descending = 1). A mean age of the population was 60 ± 10 years, with a mean body mass index of 29 ± 7 kg/m^2. Thirteen patients (72%) had known coronary risk factors such as hypertension (n = 6), diabetes (n = 4), smoking (n = 3), pre-existing coronary artery disease (n = 4), or a combination thereof. All coronary bifurcations had atherosclerotic plaques. Plaque types were thin-cap fibroatheroma (n = 2), fibroatheroma with or without calcification (n = 11, with or without = 5 of 6), and fibrocalcific plaques (n = 13).

The mean longitudinal length of the proximal segment in the main vessel to the branch point was 7.2 ± 3.0 mm, and the distance from branch point to the distal end of the stented segment was 6.7 ± 2.8 mm. Plaque thickness was the greatest on the lateral wall in the distal main vessel (1.3 ± 0.7 mm), followed by the lateral wall in the proximal main vessel (1.1 ± 0.7 mm). All lateral walls showed significantly greater intimal thickness as compared with those in the flow divider (Fig. 2). Similarly, necrotic core thickness also was significantly greater in the lateral wall versus the flow divider, where the necrotic core was

JACC Vol. 55, No. 16, 2010
April 20, 2010:1679–87

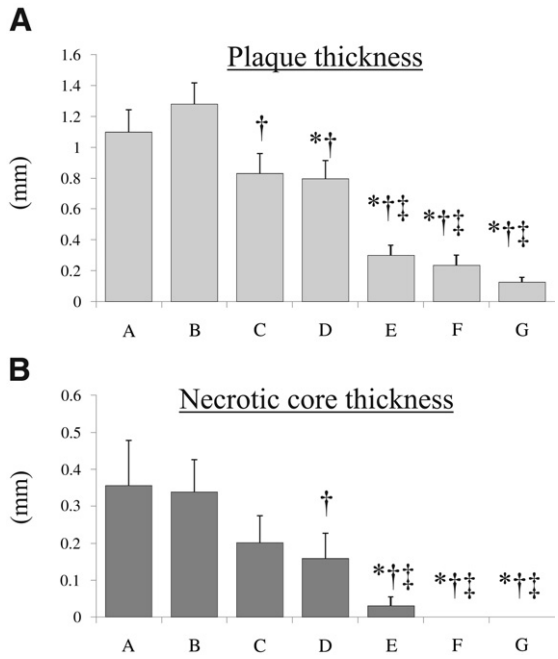

Figure 2 Distribution of Coronary Plaque in Bifurcation Lesion

Bar graphs showing the bifurcation lesions as divided into 7 regions: **(A)** thickness of the plaque (mm) in each region, **(B)** thickness of the necrotic core (mm). Low-shear areas had a higher prevalence of coronary plaque as well as necrotic core. Note that carinal region was rarely involved (G). $p < 0.05$ versus *A, versus †B, versus ‡C and D.

minimal or absent (Fig. 2). Figure 3 illustrates typical growth of necrotic core at bifurcation sites.

Stented bifurcation lesions. Forty stented bifurcation lesions (DES, n = 19; BMS, n = 21) from 40 patients with an age of 61 ± 16 years in the DES group and 58 ± 17 years in the BMS group ($p = 0.61$) were evaluated. The prevalence of males (DES, 79% vs. BMS, 62%; $p = 0.49$) and a mean implant duration (median [interquartile range IQR]: DES, 330 days [188 to 680 days] vs. BMS, 150 days [IQR 54 to 540 days]; $p = 0.14$) was similar between the 2 groups. Procedural parameters such as location of bifurcation lesions, techniques of stenting, and number of implanted stents were comparable (Table 1). Restenosis in the main vessel was significantly more frequent in BMS group as compared with the DES group (33% vs. 5%; $p = 0.046$) (Table 1). The incidence of late stent thrombosis (more than 30 days) in the main vessel was borderline significantly greater in the DES versus the BMS group (75% vs. 36%; $p = 0.06$) (Table 1, Fig. 4), whereas acute or subacute stent thrombosis (fewer than 30 days) was similar between the DES and BMS groups (Table 1). The stent duration of late stent thrombosis (more than 30 days) was significantly longer in the DES group as compared with the BMS group (270 days [IQR 195 to 585 days] vs. 60 days [IQR 35 to 105 days]; $p = 0.003$).

In patients who died within 30 days of stent implantation, the cause of death was similar between the DES and BMS groups (Table 1). Both stent groups had 4 stent-related death (DES group, 3 thrombosis and 1 coronary perforation; BMS group, 3 thrombosis and 1 coronary perforation), 2 nonstent-related cardiac deaths in each group (DES group, 1 diffuse coronary artery disease and 1 cardiogenic shock after acute myocardial infarction; BMS group, 1 diffuse coronary artery disease and 1 cardiogenic shock after acute myocardial infarction), and 1 noncardiac death in each group (DES group, 1 sepsis; BMS group, 1 sepsis). However, among the patients who died more than 30 days after stent implantation, the incidence of stent-related death was greater in patients with DES (9 of 12; 75%) as compared with those with BMS (5 of 14; 36%), but the difference remained of borderline significance because of a limited sample size. Nonstent-related death was documented in 3 patients (25%) with a DES (2 diffuse coronary artery disease and 1 severe aortic stenosis) and in 4 patients (29%) with a BMS (3 diffuse coronary artery disease and 1

Table 1 Patient, Lesion, and Procedural Characteristics and Pathologic Findings

	DES (n = 19)	BMS (n = 21)	p Value
Age (yrs)	61 ± 16	58 ± 17	0.61
Males	15 (79)	13 (62)	0.49
Mean duration (days)*	330 (188–680)	150 (54–540)	0.14
More than 30 days	12 (63)	14 (67)	> 0.99
Location			
LM/LAD/LCX	4	1	0.44
LAD/LD	10	12	
LCX/OM	4	7	
RCA/PDA	1	1	
Technique			
1 stent	10	9	0.38
2 stents: T/V/crush	5/2/2	9/3/0	
No. of stents*	2 (1–2)	2 (1–2)	0.55
Restenosis			
MV	1 (5)	7 (33)	0.046
SB	3 (16)	6 (29)	0.46
Thrombosis			
≤30 days			
MV	3/7 (43)	3/7 (43)	>0.99
SB	3/7 (43)	4/7 (57)	0.59
>30 days			
MV	9/12 (75)	5/14 (36)	0.06
SB	5/12 (42)	2/14 (14)	0.19
Timing of thrombus* (>30 days)	270 (195–585)	60 (35–105)	0.003
Cause of death			
SRD/NSRCD/NCD ≤30 days	4/2/1	4/2/1	>0.99
>30 days	9/3/0	5/4/5	0.04

Values are mean ± SD, n (%), or n. *Expressed as median (interquartile range).

BMS = bare-metal stent(s); DES = drug-eluting stent(s); LAD = left anterior descending coronary artery; LCX = left circumflex; LD = left diagonal; LM = left main; MV = main vessel; NSRCD = nonstent-related cardiac death; NCD = noncardiac death; OM = obtuse marginal; PDA = posterior descending artery; RCA = right coronary artery; SB = side branch; SRD = stent-related death; T/V = T-stenting/V-stenting.

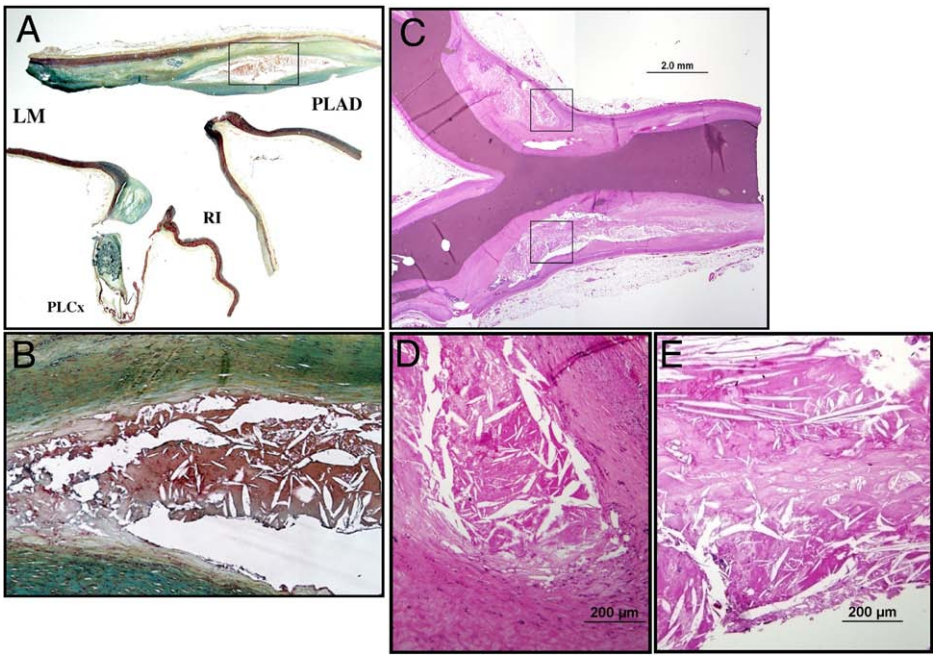

Figure 3 Representative Histologic Images of Coronary Plaque in Bifurcation Lesion

(A) Longitudinal section of trifurcation: left main (LM)/proximal left anterior descending coronary artery (PLAD)/ramus intermedicus (RI)/proximal left circumflex (PLCx). **(B)** Atherosclerotic plaques were observed in the lateral wall, whereas the flow divider regions were spared. **(C)** Longitudinal section obtained from the region of the LCx/left obtuse marginal bifurcation. Note the severe luminal narrowing proximal and distal to the bifurcation. **(D, E)** Low-shear regions show atherosclerotic plaque development, including necrotic core formation, whereas flow divider regions (the carina) have minimal intimal thickening.

acute myocardial infarction in nontreated vessel). Noncardiac death was observed in 5 patients (36%) in the BMS group (2 trauma, 1 cancer, 1 complication of surgery, and 1 cerebrovascular disease) and none in the DES group.

Pathologic assessment and morphometric analysis (stent implant duration of more than 30 days). Neointimal thickness was significantly less at the flow divider site as compared with the lateral wall in the DES group (median [interquartile range]: 0.07 mm [IQR 0.03 to 0.15 mm] vs. 0.17 mm [IQR 0.09 to 0.23 mm]; p = 0.001), whereas this difference did not reach statistical significance for BMS cases (0.26 mm [IQR 0.16 to 0.73 mm] vs. 0.44 mm [IQR 0.17 to 0.67 mm]; p = 0.25). Similarly, the percentage of uncovered struts was significantly greater at flow divider sites as compared with the lateral wall in the DES group (40% [IQR 16% to 76%] vs. 0% [IQR 0% to 15%; p = 0.001]), whereas there was no significant difference in the BMS group (0% [IQR 0% to 21%] vs. 0% [IQR 0% to 0%]: p = 0.09). Fibrin deposition also was seen frequently in flow divider sites as compared with the lateral wall (60% [IQR 21% to 67%] vs. 17% [IQR 0% to 55%]; p = 0.01) (Table 2), which was observed only in the DES group. Most of the thrombi originated at the flow divider sites, where uncovered struts were observed frequently.

The DES group showed significantly greater fibrin deposition and uncovered struts and less neointimal thickness as compared with the BMS group at flow divider sites, whereas there was no statistical significance in fibrin deposition and uncovered struts between the DES and BMS groups at the lateral wall.

Stent-induced flow disturbances. The character of flow in a stented region is governed by the flow waveform, pulsatility, and compliance mismatch. Therefore, to better examine the temporal and spatial evolution of the flow in our

Table 2 Morphometric Comparison Between Flow Divider Versus Lateral Wall in DES and BMS

	DES (12 Lesions, 17 Stents)			BMS (14 Lesions, 18 Stents)			p Value for DES vs. BMS	
	Flow Divider	Lateral	p Value	Flow Divider	Lateral	p Value	Flow Divider	Lateral
Neointimal thickness (mm)	0.07 (0.03–0.15)	0.17 (0.09–0.23)	0.001	0.26 (0.16–0.73)	0.44 (0.17–0.67)	0.25	0.0002	0.004
Fibrin deposition (% struts)	60 (21–67)	17 (0–55)	0.01	8 (0–33)	3 (0–21)	0.21	0.008	0.19
Uncovered struts (% struts)	40 (16–76)	0 (0–15)	0.001	0 (0–21)	0 (0–0)	0.10	0.004	0.38

Values are expressed as median (interquartile range).

bifurcation model and to determine the effects of a stent, 2 phases of the flow were examined. Phase 1 included peak systolic of the flow, at which flow separation of the lateral walls is known to occur. Phase 2 included early diastole, as flow begins to decelerate and become unstable.

In the nonstented bifurcation model, the flow during the peak systolic phase produced large boundary layer separation (low-shear stress) at the lateral wall, whereas the flow remained attached at the flow divider regions (high-shear stress). During the early diastolic phase, flow decelerated and reversed; however, no secondary vortical structures were observed within the carinal region. After deployment of stent, the boundary layer separation of the lateral walls was still present; however, the region of separation at the side branch had increased as compared with the nonstented model. Side branch expansion of the stent resulted in a reduction of the boundary layer separation of the side branch (Fig. 5). During the early diastolic phase, as flow decelerated, vortical flow structures were observed in the carinal region (Fig. 5H). All observations were conducted in a bifurcation model of 40° with a flow split ratio of 65:35. We acknowledge that varying the angle and flow ratio further may lead to more or fewer flow disturbances (13). Moreover, the peak flow of our model was in phase with peak systolic pressure, which differs from native coronary blood flow.

Discussion

The main findings of the present study were: 1) atherosclerotic plaques developed at bifurcation sites and were more pronounced in low shear as compared with high-shear regions (flow divider); 2) in our autopsy series, there was a greater prevalence of late stent thrombosis in bifurcation lesions treated with a DES as compared with a BMS; 3) arterial healing was impaired with greater delay at the flow divider as compared with the lateral wall sites; and 4) in the in vitro bifurcation model, flow disturbance increased after stent placement at the flow divider site.

Development of atherosclerotic plaque in bifurcation lesion. It has been reported that the occurrence of atherosclerosis at bifurcations is closely related to local

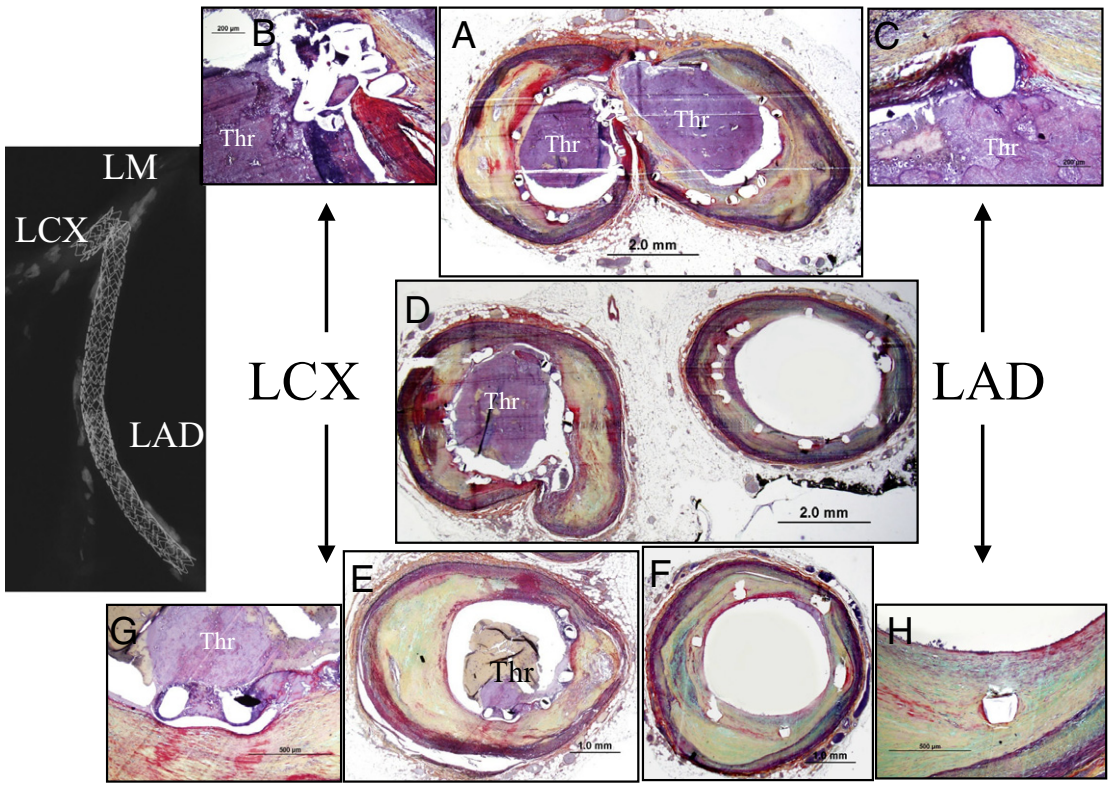

Figure 4 **A Case of Late Drug-Eluting Stent Thrombosis in Bifurcation Lesion**

A 55-year-old man with a history of smoking, hypertension, and dyslipidemia received 2 Taxus stents in the ostium of the left anterior descending coronary artery (LAD) and left circumflex (LCX), with overlapping Taxus stents placed in the LAD. The patient died suddenly 2 years after stent implantation. **(Far left)** Radiograph showed mildly calcified coronary artery. **(A)** Both stents were occluded with platelet-rich thrombus (Thr) at the ostium of the LAD and LCX. **(B, C)** High-magnification images demonstrated adherent thrombus in the region of the uncovered struts at the flow divider. **(D, E, G)** Uncovered struts and adherent thrombus also were observed in all sections of the LCX stent. **(D, F, H)** The middle to distal portion of the LAD stent showed absence of thrombus and healed luminal surface with mild neointimal thickening. LM = left main artery.

hemodynamic forces such as shear stress (1–3,14). Moreover, some autopsy studies have demonstrated a higher prevalence of atherosclerotic plaques in the low-shear regions in coronary bifurcation lesions (15,16). In the present study, we investigated the axial distribution of coronary plaques in bifurcation lesions using a longitudinal sectioning method. The lateral wall (i.e., low-shear areas) showed significantly greater prevalence of coronary plaque formation as compared with the flow divider sites (i.e., high-shear areas), which was consistent with the findings of previous studies (15,16). In addition to the plaque distribution, progressive atherosclerosis such as necrotic core formation was significantly more frequent in the lateral wall (low-shear regions).

Plaque progression is initiated by endothelial dysfunction followed by increased permeability of lipoproteins, upregulation of adhesion molecules such as intercellular adhesion molecules and vascular cell adhesion molecules, and leukocyte transmigration (4). It is well known that there is a strong correlation between endothelial dysfunction and low-shear stress and oscillatory flow, which usually is observed in the bifurcation lesions or in areas of abrupt curvatures. Cheng et al. (17) reported that upregulation of endothelial nitric oxide synthase was observed in a high-shear areas using a cast-induced increased shear stress model in the mouse carotid artery. In a later study, Cheng et al. (18) showed elevated gene expressions of interleukin-6, C-reactive protein, intercellular adhesion molecules, vascular cell adhesion molecules, and vascular endothelial growth factor in the low-shear area using the same model. Thus, shear stress seems to play an important role not only in early plaque formation, but also its progression. In addition, bifurcation angle variation also plays a central role, as shown by Perktold et al. (19): the larger the angle of bifurcation, the greater the turbulence. Moreover, the ratio of the caliber from the proximal to the distal or side branch also influences the flow turbulence (20,21). Obtaining the 3-dimensional structure of the bifurcation along with postmortem angiography results followed by digital reconstruction may be useful to understand better the detail of atherosclerotic plaque development and its spatial distribution, which was not used in the present study.

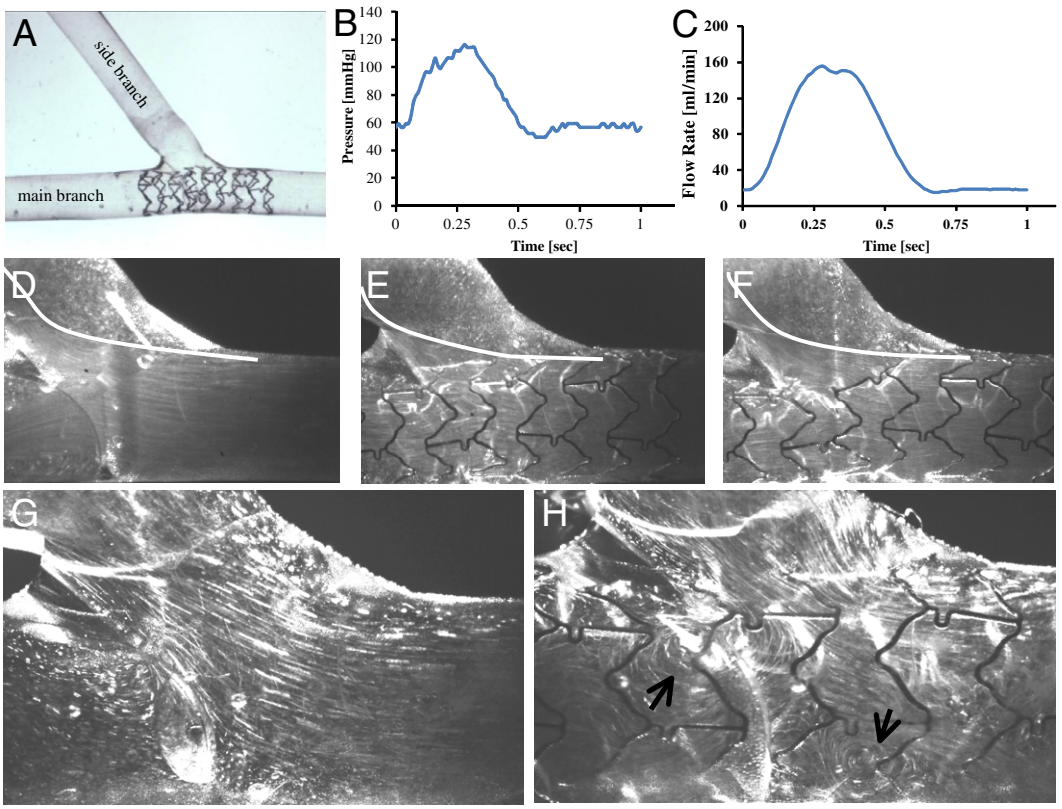

Figure 5 **Stent-Induced Flow Disturbances Within a Compliant Bifurcation Model In Vitro**

(A) Gross image of the in vitro stented bifurcation model. The **(B)** recorded pressure and **(C)** flow rate measurements are displayed and were maintained within physiologic conditions. **(D)** Boundary layer separation in the nonstented model was observed at peak systolic phase at the lateral walls, particularly at the side branch (**white line** represents boundary layer). **(E)** After stenting, the boundary layer was increased as compared with the nonstented model. **(F)** However, after side branch dilation, the boundary layer was decreased. **(G)** No flow disturbances were observed during the early diastolic phase of the cycle in the nonstented model. **(H)** However, in the stented model, vortical structures **(arrows)** were present in the carinal region.

Delayed arterial healing in the bifurcation lesion after DES implantation. Polymer-based DESs have dramatically reduced rates of restenosis and late lumen loss as compared with BMSs, according to randomized clinical pivotal trials in de novo short noncomplex lesions (22,23). Subsequently, this technology was used for a wider range of lesion morphologic features, such as bifurcation/ostial, left main coronary artery, and long lesions, which have been reported to have a high incidence of restenosis and revascularization rate (24–26). However, recent meta-analyses reported higher rates of late stent thrombosis in DESs (27–29), especially for off-label indications (30). Although we previously reported that bifurcation lesions are one of the pathologic risk factors for late stent thrombosis in both BMSs and DESs (10,31), the mechanism of late stent thrombosis in a bifurcation lesion has not been explored fully.

In the present study, although the difference remained of borderline significance because of a limited sample size, a greater incidence of late stent thrombosis was documented in the DES group as compared with the BMS group at bifurcation sites. Detailed morphometric and pathologic analysis revealed greater delayed arterial healing, as evidenced by incomplete stent coverage and fibrin deposition in bifurcation lesions stented with a DES versus a BMS. This difference was especially pronounced at the flow divider sites, where thrombi were observed to originate at the site of uncovered struts. Furthermore, our in vitro experimental bifurcation model demonstrated that deployment of stents can alter boundary layer separation of the lateral walls and can produce disturbances (vortical structures) at the carina. Regions of boundary layer separation are associated with reduced levels of wall shear stress, poor mass transfer of blood flow and vessel wall, and an increase in time residence of circulating blood elements. Moreover, the development of vortical structures can prolong and alter localized areas of low-flow regions and can influence drug deposition, arterial healing post stenting, and local fibrin and platelet deposition (32–34).

Richter et al. (20) showed that a greater neointimal formation occurs in the lateral as compared with the flow divider walls after stent implantation in a porcine iliofemoral bifurcation model, which is consistent with our finding in the present study. However, these differences were not significant in the BMS group, which may be because of more rapid healing and more uniform neointimal formation after BMS implantation. Thus, a combination of drug effect and flow disturbance both are likely to accelerate the delayed healing in bifurcation lesion.

It has been reported that deploying multiple stents (both in main vessels and side branches) to treat bifurcation lesion have higher restenosis and thrombosis rates as compared with a single stent with balloon angioplasty in the side branch (24). In the present study, we could not demonstrate significant differences between single-stent and multistent techniques in the incidence of clinical events, likely because of the small number of samples. However, because delayed arterial healing occurs in the presence of 1 stent, it seems reasonable that a multistent technique would produce, in even the best-case scenario, a similar result, as polymer and drug levels are likely to be higher. Furthermore, based on our findings of plaque distribution (i.e., predominantly distributed on the lateral wall), it may be possible to design a new stent that may cover only the lateral wall. This would minimize the risk of stent thrombosis by reducing unnecessary metals in the carinal region.

Study limitations. Because the data are derived from autopsy specimens, the results may not be representative of all patients who receive a DES and survive. Also, more aggressive approaches have been applied recently in the DES as compared with the BMS era, which may account for some stent-related death. However, to the best of our knowledge, this is the only autopsy study in which stented bifurcation lesions were studied specifically to examine the vascular responses to both a BMS and DES. It is not possible to conduct this type of analysis from clinical studies because only pathologic analysis can provide high-resolution images to determine delayed healing in various regions of the bifurcation sites. Therefore, we believe that the current study provides valuable information that furthers our understanding of vascular responses to the DES.

Conclusions

Plaque formation in native coronary bifurcations and neointimal growth after DES implantation showed substantial differences between the flow divider and the lateral wall regions. The greater prevalence of late stent thrombosis in the DES group compared with the BMS group at autopsy is likely related to an exaggerated delay of arterial healing, which may be caused primarily by flow disturbances in drug retention.

Reprints requests and correspondence: Dr. Renu Virmani, CVPath Institute, Inc., 19 Firstfield Road, Gaithersburg, Maryland 20878. E-mail: rvirmani@cvpath.org.

REFERENCES

1. Ku DN, Giddens DP, Zarins CK, Glagov S. Pulsatile flow and atherosclerosis in the human carotid bifurcation. Positive correlation between plaque location and low oscillating shear stress. Arteriosclerosis 1985;5:293–302.
2. Friedman MH, Bargeron CB, Deters OJ, Hutchins GM, Mark FF. Correlation between wall shear and intimal thickness at a coronary artery branch. Atherosclerosis 1987;68:27–33.
3. Prosi M, Perktold K, Ding Z, Friedman MH. Influence of curvature dynamics on pulsatile coronary artery flow in a realistic bifurcation model. J Biomech 2004;37:1767–75.
4. Traub O, Berk BC. Laminar shear stress: mechanisms by which endothelial cells transduce an atheroprotective force. Arterioscler Thromb Vasc Biol 1998;18:677–85.
5. Beohar N, Davidson CJ, Kip KE, et al. Outcomes and complications associated with off-label and untested use of drug-eluting stents. JAMA 2007;297:1992–2000.

6. Yamashita T, Nishida T, Adamian MG, et al. Bifurcation lesions: two stents versus one stent—immediate and follow-up results. J Am Coll Cardiol 2000;35:1145–51.
7. Al Suwaidi J, Berger PB, Rihal CS, et al. Immediate and long-term outcome of intracoronary stent implantation for true bifurcation lesions. J Am Coll Cardiol 2000;35:929–36.
8. Iakovou I, Schmidt T, Bonizzoni E, et al. Incidence, predictors, and outcome of thrombosis after successful implantation of drug-eluting stents. JAMA 2005;293:2126–30.
9. Farb A, Weber DK, Kolodgie FD, Burke AP, Virmani R. Morphological predictors of restenosis after coronary stenting in humans. Circulation 2002;105:2974–80.
10. Joner M, Finn AV, Farb A, et al. Pathology of drug-eluting stents in humans: delayed healing and late thrombotic risk. J Am Coll Cardiol 2006;48:193–202.
11. Finn AV, Joner M, Nakazawa G, et al. Pathological correlates of late drug-eluting stent thrombosis: strut coverage as a marker of endothelialization. Circulation 2007;115:2435–41.
12. Yazdani SK, Moore JE Jr., Berry JL, Vlachos PP. DPIV measurements of flow disturbances in stented artery models: adverse affects of compliance mismatch. J Biomech Eng 2004;126:559–66.
13. Liepsch D, Pflugbeil G, Matsuo T, Lesniak B. Flow visualization and 1- and 3-D laser-Doppler-anemometer measurements in models of human carotid arteries. Clin Hemorheol Microcirc 1998;18:1–30.
14. Kimura BJ, Russo RJ, Bhargava V, McDaniel MB, Peterson KL, DeMaria AN. Atheroma morphology and distribution in proximal left anterior descending coronary artery: in vivo observations. J Am Coll Cardiol 1996;27:825–31.
15. Fox B, James K, Morgan B, Seed A. Distribution of fatty and fibrous plaques in young human coronary arteries. Atherosclerosis 1982;41:337–47.
16. Grottum P, Svindland A, Walloe L. Localization of atherosclerotic lesions in the bifurcation of the main left coronary artery. Atherosclerosis 1983;47:55–62.
17. Cheng C, van Haperen R, de Waard M, et al. Shear stress affects the intracellular distribution of eNOS: direct demonstration by a novel in vivo technique. Blood 2005;106:3691–8.
18. Cheng C, Tempel D, van Haperen R, et al. Atherosclerotic lesion size and vulnerability are determined by patterns of fluid shear stress. Circulation 2006;113:2744–53.
19. Perktold K, Peter RO, Resch M, Langs G. Pulsatile non-Newtonian blood flow in three-dimensional carotid bifurcation models: a numerical study of flow phenomena under different bifurcation angles. J Biomed Eng 1991;13:507–15.
20. Richter Y, Groothuis A, Seifert P, Edelman ER. Dynamic flow alterations dictate leukocyte adhesion and response to endovascular interventions. J Clin Invest 2004;113:1607–14.
21. Lee SW, Antiga L, Spence JD, Steinman DA. Geometry of the carotid bifurcation predicts its exposure to disturbed flow. Stroke 2008;39:2341–7.
22. Moses JW, Leon MB, Popma JJ, et al. Sirolimus-eluting stents versus standard stents in patients with stenosis in a native coronary artery. N Engl J Med 2003;349:1315–23.
23. Stone GW, Ellis SG, Cox DA, et al. A polymer-based, paclitaxel-eluting stent in patients with coronary artery disease. N Engl J Med 2004;350:221–31.
24. Colombo A, Moses JW, Morice MC, et al. Randomized study to evaluate sirolimus-eluting stents implanted at coronary bifurcation lesions. Circulation 2004;109:1244–9.
25. Park SJ, Kim YH, Lee BK, et al. Sirolimus-eluting stent implantation for unprotected left main coronary artery stenosis: comparison with bare metal stent implantation. J Am Coll Cardiol 2005;45:351–6.
26. Kim YH, Park SW, Lee SW, et al. Sirolimus-eluting stent versus paclitaxel-eluting stent for patients with long coronary artery disease. Circulation 2006;114:2148–53.
27. Daemen J, Wenaweser P, Tsuchida K, et al. Early and late coronary stent thrombosis of sirolimus-eluting and paclitaxel-eluting stents in routine clinical practice: data from a large two-institutional cohort study. Lancet 2007;369:667–78.
28. Lagerqvist B, James SK, Stenestrand U, Lindback J, Nilsson T, Wallentin L. Long-term outcomes with drug-eluting stents versus bare-metal stents in Sweden. N Engl J Med 2007;356:1009–19.
29. Stone GW, Moses JW, Ellis SG, et al. Safety and efficacy of sirolimus- and paclitaxel-eluting coronary stents. N Engl J Med 2007;356:998–1008.
30. Farb A, Boam AB. Stent thrombosis redux—the FDA perspective. N Engl J Med 2007;356:984–7.
31. Farb A, Burke AP, Kolodgie FD, Virmani R. Pathological mechanisms of fatal late coronary stent thrombosis in humans. Circulation 2003;108:1701–6.
32. Brown CH 3rd, Leverett LB, Lewis CW, Alfrey CP Jr., Hellums JD. Morphological, biochemical, and functional changes in human platelets subjected to shear stress. J Lab Clin Med 1975;86:462–71.
33. Balakrishnan B, Tzafriri AR, Seifert P, Groothuis A, Rogers C, Edelman ER. Strut position, blood flow, and drug deposition: implications for single and overlapping drug-eluting stents. Circulation 2005;111:2958–65.
34. Kolachalama VB, Tzafriri AR, Arifin DY, Edelman ER. Luminal flow patterns dictate arterial drug deposition in stent-based delivery. J Control Release 2009;133:24–30.

Key Words: atherosclerosis ■ bifurcation ■ drug-eluting stent ■ flow disturbance.